Dynamics of a short cavity swept source OCT laser

S. Slepneva,[1,2] **B. O'Shaughnessy,**[1,2] **B. Kelleher,**[1,2] **S.P. Hegarty,**[1,2] **A. Vladimirov,**[3] **H.-C. Lyu,**[4] **K. Karnowski,**[4] **M. Wojtkowski,**[4] **G. Huyet**[1,2]

[1] *Centre for Advanced Photonics and Process Analysis & Department of Applied Physics and Instrumentation, Cork Institute of Technology, Cork, Ireland*

[2] *Tyndall National Institute, University College Cork, Lee Maltings, Dyke Parade, Cork, Ireland*

[3] *Weierstrass Institute for Applied Analysis and Stochastics, Mohrenstrasse 39, D-10117 Berlin, Germany*

[4] *Institute of Physics, Faculty of Physics, Astronomy and Informatics, Nicolaus Copernicus University, Grudziadzka 5, PL-87-100 Torun, Poland*

*bryan.kelleher@tyndall.ie

Abstract: We investigate the behaviour of a short cavity swept source laser with an intra cavity swept filter both experimentally and theoretically. We characterise the behaviour of the device with real-time intensity measurements using a fast digital oscilloscope, showing several distinct regimes, most notably regions of mode-hopping, frequency sliding mode-locking and chaos. A delay differential equation model is proposed that shows close agreement with the experimental results. The model is also used to determine important quantities such as the minimum and maximum sweep speeds for the mode-locking regime. It is also shown that by varying the filter width the maximum sweep speed can be increased but at a cost of increasing the instantaneous linewidth. The consequent impacts on optical coherence tomography applications are analysed.

OCIS codes: (140.3600) Lasers, tunable; (140.3430) Laser theory; (110.4500) Optical coherence tomography.

References and links

1. A. Bilenca, S. H. Yun, G. J. Tearney, and B. Bouma, "Numerical study of wavelength-swept semiconductor ring lasers: the role of refractive-index nonlinearities in semiconductor optical amplifiers and implications for biomedical imaging applications," Opt. Lett. **31**, 760–762 (2006).
2. D. Huang, E. A. Swanson, C. P. Lin, J. S. Schuman, W. G. Stinson, W. Chang, M. R. Hee, T. Flotte, K. Gregory, C. A. Puliafito et al., "Optical coherence tomography," Science **254**, 1178–1181 (1991).
3. E. A. Swanson, J. Izatt, M. R. Hee, D. Huang, C. Lin, J. Schuman, C. Puliafito, and J. G. Fujimoto, "In vivo retinal imaging by optical coherence tomography," Optics letters **18**, 1864–1866 (1993).
4. V. Farooq, B. D. Gogas, T. Okamura, J. H. Heo, M. Magro, J. Gomez-Lara, Y. Onuma, M. D. Radu, S. Brugaletta, G. van Bochove et al., "Three-dimensional optical frequency domain imaging in conventional percutaneous coronary intervention: the potential for clinical application," European heart journal **34**, 875–885 (2013).
5. Y. Nakajima, Y. Shimada, A. Sadr, I. Wada, M. Miyashin, Y. Takagi, J. Tagami, and Y. Sumi, "Detection of occlusal caries in primary teeth using swept source optical coherence tomography," Journal of Biomedical Optics **19**, 016020–016020 (2014).
6. B. H. Lee, E. J. Min, and Y. H. Kim, "Fiber-based optical coherence tomography for biomedical imaging, sensing, and precision measurements," Optical Fiber Technology **19**, 729–740 (2013).
7. M. A. Choma, M. V. Sarunic, C. Yang, and J. A. Izatt, "Sensitivity advantage of swept source and Fourier domain optical coherence tomography," Optics Express **11**, 2183–2189 (2003).
8. T. Klein, W. Wieser, L. Reznicek, A. Neubauer, A. Kampik, and R. Huber, "Multi-MHz retinal OCT," Biomedical Optics Express **4**, 1890–1908 (2013).

#210492 - $15.00 USD Received 6 May 2014; revised 28 Jun 2014; accepted 30 Jun 2014; published 21 Jul 2014

9. R. Huber, M. Wojtkowski, and J. G. Fujimoto, "Fourier Domain Mode Locking (FDML): A new laser operating regime and applications for optical coherence tomography," Opt. Express **14**, 3225–3237 (2006).
10. M. Kuznetsov, W. Atia, B. Johnson, and D. Flanders, "Compact ultrafast reflective Fabry-Perot tunable lasers for OCT imaging applications," in "BiOS," (International Society for Optics and Photonics, 2010), pp. 75541F–75541F.
11. I. Grulkowski, J. J. Liu, B. Potsaid, V. Jayaraman, C. D. Lu, J. Jiang, A. E. Cable, J. S. Duker, and J. G. Fujimoto, "Retinal, anterior segment and full eye imaging using ultrahigh speed swept source oct with vertical-cavity surface emitting lasers," Biomedical Optics Express **3**, 2733 (2012).
12. E. Avrutin and L. Zhang, "Dynamics of semiconductor lasers under fast intracavity frequency sweeping," in Transparent Optical Networks (ICTON), 2012 14th International Conference on, (IEEE, 2012), pp. 1–4.
13. W. Atia, M. Kuznetsov, and D. Flanders, "Linearized swept laser source for optical coherence analysis system," (2009). US Patent App. 12/027,710.
14. B. Johnson and D. Flanders, "Laser swept source with controlled mode locking for OCT medical imaging," (2013). EP Patent App. EP20,110,808,812.
15. S. Slepneva, B. Kelleher, B. O'Shaughnessy, S.P. Hegarty, A. Vladimirov, and G. Huyet, "Dynamics of Fourier domain mode-locked lasers," Opt. Express **21**, 19240–19251 (2013).
16. A.G. Vladimirov and D. Turaev, "Model for passive mode-locking in semiconductor lasers," Phys. Rev. A **72**, 033808 (2005).
17. A. Vladimirov, D. Turaev, and G. Kozyreff, "Delay differential equations for mode-locked semiconductor lasers," Opt. Lett. **29**, 1221–1223 (2004).
18. A.G. Vladimirov and D. Turaev, "A new model for a mode-locked semiconductor laser," Radiophys. and Quantum Electronics **47**, 769–776 (2004).
19. C. Jirauschek, B. Biedermann and R. Huber, "A theoretical description of Fourier domain mode locked lasers,", Opt. Express **17**, 24013?24019 (2009).
20. R. Huber, M. Wojtkowski, K. Taira and J.G. Fujimoto, "Amplified, frequency swept lasers for frequency domain reflectometry and OCT imaging: design and scaling principles," Opt. Express **13**, 3513–3528 (2005).

1. Introduction

Optical Coherence Tomography (OCT) is an imaging technique that enables the acquisition of high-resolution, cross-sectional, real-time images of scattering media that are transparent in the near-infrared range [2]. OCT is best known as a clinical diagnostic tool, typically used for monitoring the eye [3] but the field of its application has expanded greatly in recent years [4–6].

By introducing Fourier domain techniques, dramatic increases in speed and sensitivity have been achieved compared to the previously developed time domain techniques [7]. In particular, Swept Source (SS) Fourier domain OCT techniques show the highest acquisition speeds today [8]. Typically in such a system one has an optical spectrum of $>$100 nm width swept out at a high frequency rate ($\sim$ hundreds of kHz to MHz), with a narrow instantaneous spectrum due to the narrow filter. Continuous improvements in the performance of SS-OCT systems have been possible due to the development of novel swept sources such as Fourier Domain Mode-locked Lasers (FDMLs) [9], compact frequency swept sources [10] and tunable VCSELs [11]. Ideally for OCT one desires both a wide spectrum and a regular, coherent, dynamic behavior so as to maximise both axial resolution and imaging depth.

In this work we analyze both experimentally and theoretically, the performance of a short cavity ($\sim$ 10 cm) laser with swept intra-cavity filtering. While some experimental observations [13, 14] and theoretical descriptions [12] of the properties of this system have been reported there has not been a direct comparison of a theoretical model with experimental results. It is known that the linewidth enhancement factor, the sweep speed, the length of the laser cavity and the filter width all contribute to different operation regimes such as longitudinal mode hopping and quasiperiodic pulsations [10, 12–14]. Nonetheless, the general operational principles and figures of merit such as the maximum sweep speed of these type of lasers are yet to be fully understood. The experimental analysis is carried out using a commercially available Axsun laser similar to that presented in [10,13]. The theoretical analysis is based on a delay differential equation model describing the temporal evolution of the electric field and carrier density within the laser cavity. The periodic variation of the sweeping rate induces the appearance of multiple

#210492 - $15.00 USD Received 6 May 2014; revised 28 Jun 2014; accepted 30 Jun 2014; published 21 Jul 2014

dynamical regimes. In short, at very low frequency sweeping rates the laser displays mode hopping while at sufficiently high sweeping rates a mode mixing mechanism enables pulsed laser emission. The latter case can lead to the appearance of either a periodic pulse train or a non-periodic pulse train, depending on the direction of the frequency sweep.

2. Experimental results

The laser cavity incorporated a semiconductor optical amplifier (SOA) as the gain medium. The reflective facets required for lasing were a tunable reflective filter at one end and a partially reflective mirror at the other. These were connected to the SOA via optical fibers giving a total cavity length of approximately 10 cm. The laser operated at a central wavelength of 1307 nm and a spectral width of 104nm swept out at a sweep rate of $\sim$ 50 kHz. The average output power was 35 mW directly from the laser. In order to avoid back reflections, a fiber optical isolator with 42 dB peak isolation was placed after the laser output.

We analysed the laser output in the time domain with a DC-coupled 12 GHz photoreceiver (Newport, 1554-B) and a real time oscilloscope of 12 GHz bandwidth. The spectral behaviour of the system was analysed using an optical spectrum analyzer (OSA, AQ6317B) with a resolution of 15 pm and with an electrical spectrum analyzer of 26 GHz bandwidth. The optical spectrum is shown in Fig.1.

In order to match the dynamical behaviour with the spectral position (and thus sweep speed and direction) the laser's output was mixed with a tunable laser source (TLS) of 100 kHz linewidth and the resulting intensity observed on the oscilloscope. This resulted in one "beating" section in the intensity per sweep direction per round-trip where the frequency difference between the two lasers was within the oscilloscope bandwidth. Then by varying the wavelength of the tunable laser source the beating region could be moved across the full round-trip thereby allowing reconstruction of the temporal evolution of the optical wavelength of the swept source as presented in Fig.1. The inset shows the average optical spectrum as measured on the OSA. The wavelength increased from its minimum to maximum value in 12 μs with the sweep rate exceeding 1 THz/μs and remaining almost constant along the majority of the forward wavelength sweep. The backward wavelength sweep had a duration of approximately 8 μs. (In fact, in the most modern Axsun lasers, the SOA is switched off during the backward sweep since it results in poor imaging performance relative to the forward sweep. The reasons for this will be addressed later in the manuscript.) As seen in Fig. 1, the sweep is not symmetric. This

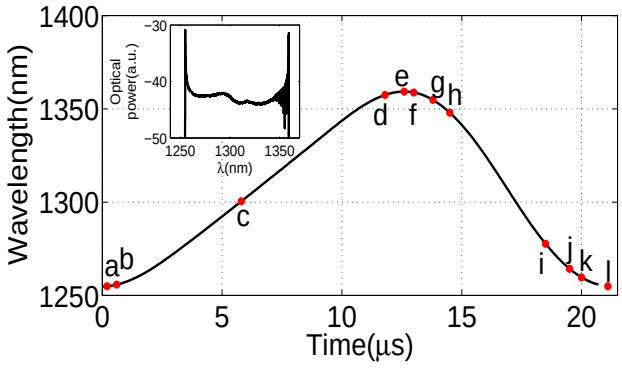

Fig. 1. The evolution of the central wavelength of the output. Plots of the intensity at the marked points are shown in Fig. 2. The inset shows the optical spectrum as measured on the OSA.

#210492 - $15.00 USD Received 6 May 2014; revised 28 Jun 2014; accepted 30 Jun 2014; published 21 Jul 2014

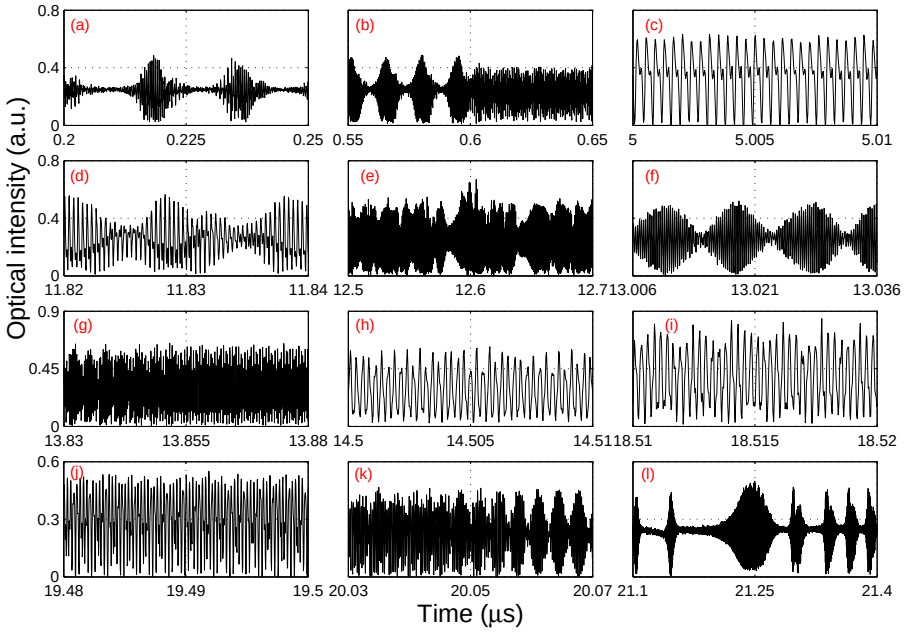

Fig. 2. Representative intensity traces. Sub-figure labels (a), (b) (c) etc. correspond to the points with the same labels in Fig. 1

asymmetry suggests that the intensity dynamics will also display an asymmetry. Further to this, we find that there is an inherent asymmetry related to the sweep-direction as previously found with FDMLs [1, 9, 15], although the dynamics in this case are quite different to those observed in the FDML system. The sequence of the dynamical regimes observed experimentally within one period of the filter sweep is shown in Fig. 2, with the sub-figure labels corresponding to the points marked on Fig. 1. Let us consider first the forward part of the wavelength sweep; that is, points (a) through (e) in Fig. 2. At (a), near the turning point of the sweep where the wavelength is changing very slowly, the output moves from one quasi-constant output to another separated by a transient pulse packet. We interpret this as a mode-hopping phenomenon and more evidence supporting this is given below and in Fig. 3. As the sweep speed increased the pulse packets moved closer together and finally merged, close to (b). For the next part of the sweep (between (b) and (d)) the sweep rate was almost constant. In this region we observed approximately periodic pulsations with a period close to the roundtrip time of the laser cavity as shown in (c). This behaviour is reminiscent of mode-locking and we interpret it as such. We will address this in more detail in the theoretical section below. Finally, close to the upper turning point ((d), (e) and (f)) a mode hopping was again observed. For the backward sweep, the behaviour at point (g) shows the transition between mode-hopping and the chaotic pulse-train shown in (h), (i) and (j) where the sweep rate is at its highest. In (k) we see the transition from chaos back to mode-hopping and finally, close to the bottom turning point we find again a mode-hopping dynamic in (l).

By mixing the output with the TLS again, we could analyze the frequency behaviour in the mode-hopping regime. We measured simultaneously the intensity of the solitary laser and the mixed intensity. Fast Fourier transforms of the mixed intensity then allowed us to recover the

#210492 - $15.00 USD Received 6 May 2014; revised 28 Jun 2014; accepted 30 Jun 2014; published 21 Jul 2014

frequency of the output relative to the TLS. Figure 3 shows the result: we see that the output is jumping from one constant frequency to another, thereby confirming the interpretation. Note however that the mode hopping need not take place between two consecutive modes.

Figure 4 shows zooms of three significant regions: a mode-hopping regime at slow sweep speed, the periodic pulse train from the forward sweep and the chaotic output from the backward sweep. In the next section we will describe a model that can assist in the interpretation of this data.

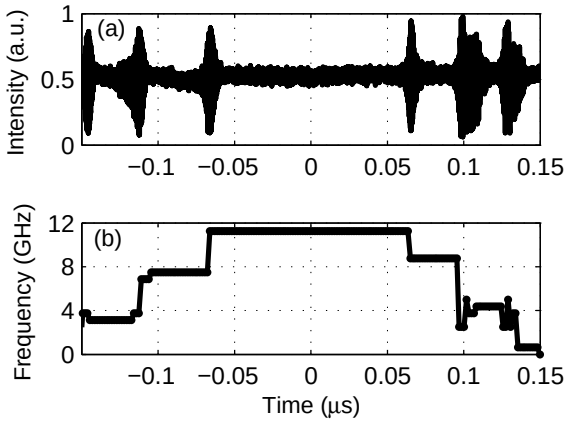

Fig. 3. Laser dynamics at low filter speed. The zero point on the time axis corresponds to the change of the sweep direction at 1255nm. (a) Intensity and (b) evolution of the beating frequency. The y-axis in (b) shows the frequency of the output relative to the frequency of the TLS.

3. Model description and simulation

3.1. Model equations

For theoretical modelling of the frequency swept laser we use the following set of delay differential equations (DDE) for the electric field envelope A and the saturable gain G of the SOA in the semiconductor amplifier:

$$\partial_t A - i\Delta(t)A + \Gamma A = \Gamma\sqrt{\kappa}e^{(1-i\alpha)G(t-T)/2}A(t-T), \tag{1}$$

$$\partial_t G = \gamma\left[g_0 - G - \left(e^G - 1\right)|A|^2\right], \tag{2}$$

where α is the linewidth enhancement factor, κ is the attenuation factor describing nonresonant linear cavity losses per round trip, T is the cold cavity round trip time, γ is the carrier density relaxation rate, and g_0 is the pump parameter. The time dependent parameter $\Delta(t)$ stands for the central frequency of the swept filter with a bandwidth Γ. The model equations (1) and (2) are similar to those used earlier to describe the dynamics of the FDML system [15]. These equations have been obtained by excluding the equation for the saturable absorption from the DDE model of a passively mode-locked semiconductor laser [16–18]. Substituting $A = a\exp\left[i\int_0^t \Delta(\tau)d\tau\right]$, where a is the electric field envelope in the frequency frame of the filter, into Eqs. (1) and (2) we obtain:

$$\partial_t a + \Gamma a = \Gamma\sqrt{\kappa}e^{(1-i\alpha)G(t-T)/2 + i\int_t^{t-T}\Delta(\tau)d\tau}a(t-T), \tag{3}$$

#210492 - $15.00 USD Received 6 May 2014; revised 28 Jun 2014; accepted 30 Jun 2014; published 21 Jul 2014

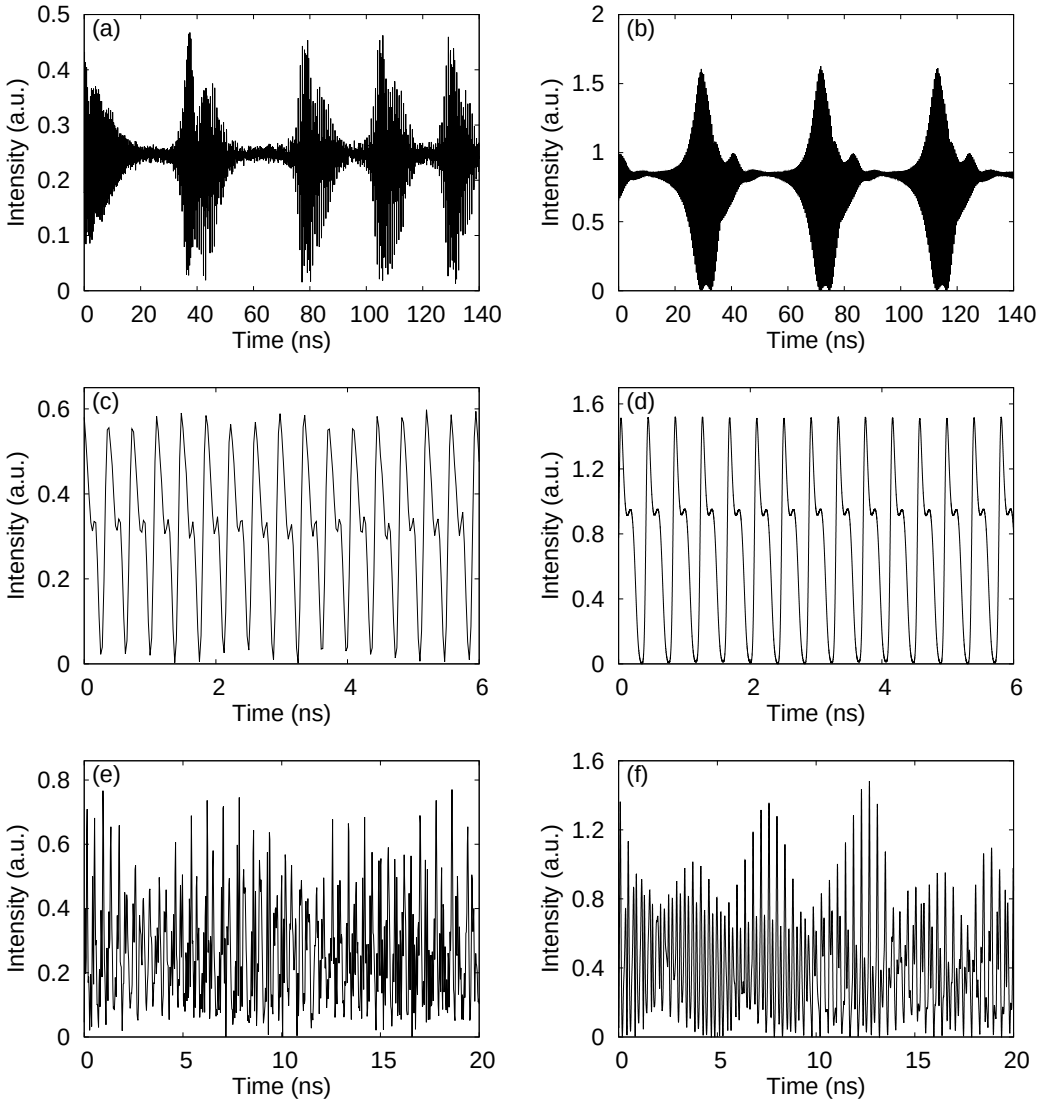

Fig. 4. Figures on the left are experimental. Figures on the right are numerical. (a) and (b) show zooms of mode-hopping behaviour close to the turning point at a sweep-speed of -0.1 GHz/ns; (c) and (d) show zooms of the periodic pulse train from the forward part of the wavelength sweep at a sweep-speed of -1 GHz/ns; (e) and (f) show zooms of the chaotic output from the backward part of the sweep at a sweep-speed of 1.3 GHz/ns.

$$\partial_t G = \gamma \left[g_0 - G - \left(e^G - 1 \right) |a|^2 \right]. \tag{4}$$

To analyse the dynamics we consider the sweep to be piecewise linear and for each simulation consider a constant sweep speed $\Delta(t) = vt$. (From Fig. 1 it is clear that such an approach is reasonable.) Then the integral in Eq. (3) becomes $\int_t^{t-T} \Delta(\tau) d\tau = vTt + vT^2/2$, where the second term describes a constant phase shift and can be omitted without loss of generality. Thus,

#210492 - $15.00 USD Received 6 May 2014; revised 28 Jun 2014; accepted 30 Jun 2014; published 21 Jul 2014

finally we get the equation

$$\partial_t a + \Gamma a = \Gamma\sqrt{\kappa} e^{(1-i\alpha)G(t-T)/2 - ivTt} a(t-T), \tag{5}$$

replacing Eq. (3). The model equations (4) and (5) were then simulated numerically at different sweep speeds and directions determined by the absolute value and the sign of the parameter v, respectively.

3.2. Numerical results

The parameters used in the simulations are given in Table 1. Figure 4 shows three simulated time-series and the corresponding experimental figures. The agreement between the experiment and numerical traces is clear. It is noteworthy that the same model has also been successfully employed to analyse the dynamics of FDMLs in [15] and so, despite the very different cavity lengths (the ratio of the lengths is of the order of 10^5), the DDE model can be used to successfully describe the dynamics in both of these swept-source configurations.

Table 1. Parameter values for simulations

Parameter	Description	Value
γ	Carrier relaxation rate	1 GHz
Γ	Filter width	15 GHz
T	Cavity round trip time	0.4 ns
κ	Linear attenuation factor	0.2
α	Linewidth enhancement factor	3.0
g_0	Unsaturated gain per round trip	3.0

As well as reproducing the experimentally observed behaviour of the system, the model can also be used for the interpretation of the operation regimes and their potential optimization. Firstly, we can try to understand the process by which the sliding mode-locking arises in the laser. The mode-hopping at low sweep speeds can be easily understood. For a static filter the output would be a CW solution as was demonstrated in [15]. Thus, for very slow tuning, one can expect the output to hop from one CW solution to the next, similar to the behaviour of the FDML device operating in the forward wavelength sweep regime [15]. The transient behaviour between the two CW solutions involves a pulse packet with a dominant time-scale of the cavity round trip time. Thus, we understand the transient behaviour as the destabilisation of one mode and the subsequent relaxation into another one. As the sweep speed is increased the time spent in each mode decreases. However, since the duration of the transient is always of the same order of magnitude, the time between successive transients is ever decreasing and eventually two successive transients merge. At this point a new phenomenon can arise. When transients are well separated, each of them consists primarily of one or two wavelengths: the dying unstable mode and the stable mode being born. However, when two transients merge with the increase of the sweep rate, new frequencies can become excited before the old ones disappear from the cavity. As a result four-wave mixing and a coherence transfer between different modes appears. Thus, a mode-locking mediated by such a mixing becomes possible. This results in a periodic pulse train for the forward sweep. Of course, the central wavelength of the spectrum at any instant is changing and so we have a sliding frequency mode-locking. For the backward sweep, much of the physics is the same. However, it manifestly does not result in a periodic output intensity. This asymmetry can be attributed to the presence of the non-zero α factor in the model equations, and is similar to the asymmetry observed in the FDML system [15, 19].

#210492 - $15.00 USD Received 6 May 2014; revised 28 Jun 2014; accepted 30 Jun 2014; published 21 Jul 2014

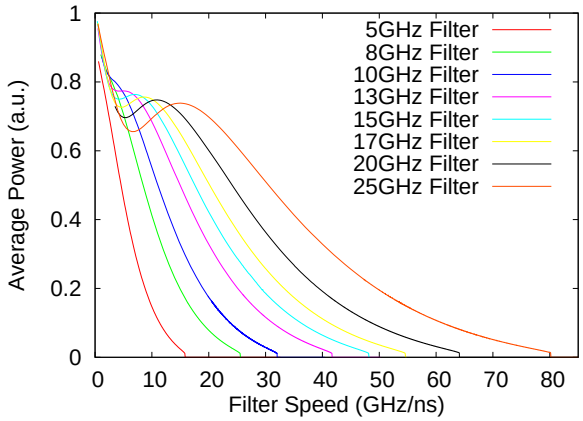

Fig. 5. Numerically simulated average output power versus sweep speed for different filter-widths.

Since the duration of the transient and the frequency swept by the filter between two successive hops are approximately constant in the mode-hopping regime (Fig. 4 (a) and (b)), we can make a physical approximation of the minimal sweep speed required for mode-locking. The sweep rate required for mode-locking must be bounded by that required for the merging of two transients: that is, when the duration of a transient towards some stable CW solution is of the same order as the time required for the filter to move as far as the destabilising point of this solution. We thus approximate the minimum sweep-speed for mode-locking $(df/dt)_{min}$ as the ratio of the frequency sweep between two successive transients Δf and the duration of the transient Δt. Despite the simplicity of this argument, the result is approximately correct and is borne out by simulations as mode-locking does not arise until (at least) the transients merge.

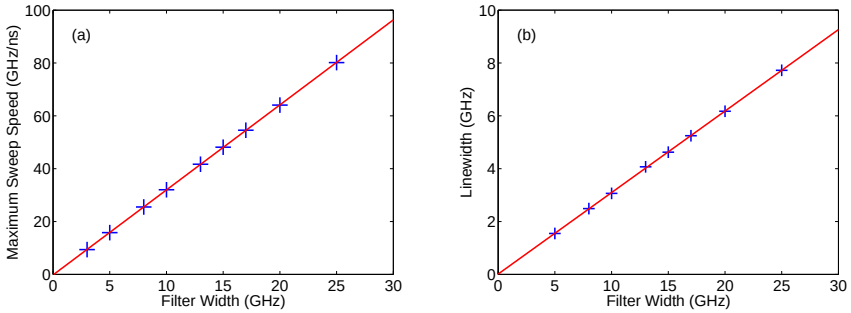

Fig. 6. (a) Numerically simulated maximum sweep-speed versus filter width and best-fit line. (b) Numerically simulated linewidth for an average output power of 0.6 (a.u.) versus filter width and best fit line.

Figure 5 shows a plot of the average laser output power versus sweep speed for various filter widths. This plot has a very distinctive shape, with maximum average power for a static filter, a steady drop in power followed by a subsequent rise to a local maximum and a gradual drop in power and eventually a switch-off of lasing emission. (Note that the mode-hopping behaviour disappears at approximately 1 GHz/ns so for the majority of each curve the y-axis shows the average mode-locked power, including the local maximum in each curve.) Another simple physical argument leads to an estimation of the maximum sweep speed at which mode-

#210492 - $15.00 USD Received 6 May 2014; revised 28 Jun 2014; accepted 30 Jun 2014; published 21 Jul 2014

locking regime still possible. Let us assume that the sweep speed is sufficiently fast so that the shift of the central frequency of the swept filter in one cavity round-trip time is larger than the filter width. (This is the so-called "Single roundtrip – post filtering limit" described in [20].) Thus, the maximum sweep speed must be limited by the ratio of the filter width and the cavity round-trip time and to a first approximation can be estimated by this ratio. In fact, it is clear that this cannot be exactly the limit since wave mixing can compensate for some of the losses induced and so the filter may move slightly faster while maintaining lasing operation. Fig. 6 (a) shows a plot of the maximum speed versus the filter width. The graph is clearly well approximated by a line. From the naive reasoning above one would find a slope of 2.5 ns^{-1} whereas the slope of the line found is ~ 3 $/ns^{-1}$. Thus, as expected, the filter can move slightly faster than the simple estimate due to extra effects such as the wave mixing. Nonetheless, despite the naivety of the reasoning, the proposed approximation works quite well.

Thus, one can access faster sweep-speeds by increasing the filter width. However, as the filter width is increased the width of the optical spectrum also increases. To quantify this change we consider a fixed average power in the output and then find the corresponding sweep speed for different filter widths from Fig. 5. We then compute the linewidth of the instantaneous spectrum defined as the square root of the second moment of the optical spectrum. As seen in Fig. 6 (b), the linewidth increases linearly. The combination of this result with the previous result on the maximum sweep speed leads to an important conclusion with regard to applications. By changing the filter width one can increase the maximum sweep speed but this comes at the cost of an increased instantaneous linewidth. Thus one must trade off the benefits of one against the other. Since the instantaneous linewidth influences the sensitivity roll-off in OCT one must thus also trade off between sweep speed and OCT image quality.

4. Conclusions

We have analysed the dynamical behaviour of a short cavity swept source laser experimentally and theoretically. The output of such a device displays an asymmetry in the sweep direction. For slow sweep speeds in either direction mode hopping between stable CW outputs takes place. For sufficiently high sweep speeds in the increasing wavelength part of the sweep, the output is a sliding frequency mode-locking mediated by non-linear wave-mixing. For decreasing wavelengths the corresponding output is a chaotic pulse train mediated by the same nonlinear mechanism. Simple arguments leading to estimations of both the minimum and maximum sweep speeds for the sliding mode-locking regime were validated by numerical simulations. Finally, it was shown that by increasing the filter width one can increase the maximum sweep speed. However, this comes with the price of an increased instantaneous linewidth and so one must weigh the accrued benefits of the two quantities against each other particularly for OCT applications.

Acknowledgments

This work was conducted under the framework of the Irish Government's Programme for Research in Third Level Institutions Cycle 5, National Development Plan 2007-2013 via the INSPIRE programme with the assistance of the European Regional Development Fund. The authors also gratefully acknowledge the support of Science Foundation Ireland under Contract No. 07/IN.1/1152 and the EU FP7 Marie Curie Action FP7-PEOPLE-2010-ITN through the PROPHET project, Grant No. 264687. A.G.V. gratefully acknowledges the support of the Science Foundation Ireland E.T.S. Walton Visitors Award Programme under Contract No. 11/W.1/I2073 and SFB 787 of the DFG. K.K. and M.W. acknowledge the support of the TEAM project financed by the European Union within the framework of the Innovative Economy programme coordinated by the Foundation for Polish Science.

#210492 - $15.00 USD Received 6 May 2014; revised 28 Jun 2014; accepted 30 Jun 2014; published 21 Jul 2014